FFT Size Optimization for LTE RoF in Nonlinear Fibre Propagation

T. Kanesan[1], *Student Member*, *IEEE*, W. P. Ng[1], *Senior Member*, *IEEE*, Z. Ghassemlooy[1], *Senior Member*, *IEEE* and C. Lu[2], *Member, IEEE*

[1]Optical Communications Research Group, NCRLab, School of CEIS, Northumbria University, Newcastle upon Tyne, U.K.

[2]Photonics Research Center, Department of Electronics and Information Engineering, The Hong Kong Polytechnic University, Hung Hom, Kowloon, Hong Kong.

Email: Thavamaran.Kanesan@northumbria.ac.uk

***Abstract*—This papers investigates the performance of the fast Fourier transform (FFT) sizes- 64, 128, 256, 512 and 1024 for the orthogonal frequency division multiplexing (OFDM) scheme in 3rd generation partnership program (3GPP)-long term evolution (LTE) and LTE-Advanced (LTE-A). This paper aims to optimize the FFT sizes with respect to quadrature phase shift keying (QPSK), 16, 64 and 256-quadrature amplitude modulation (QAM). This optimization is for the transmission of LTE signals between eNodeB (eNB) and relay node (RN) to extend the mobile coverage employing radio-over-fibre (RoF). This paper will take into account the positive frequency chirp (PFC) induced by distributed feedback laser (DFB) through direct modulation with chromatic dispersion (CD) and self phase modulation (SPM) impairments into consideration. We present the optimum optical launch power (OLP) region termed as the intermixing region between linear and nonlinear optical fibre propagation. The optimum OLP in this investigation takes place at -4 dBm which falls within the intermixing region. At the transmission rate of 200, 400, 600 and 800 Mb/s of QPSK, 16, 64 and 256-QAM, the FFT size-128 provides the optimum power penalty with average system efficiency with respect to FFT size-64 is 54% and FFT size-256 is 65%.**

***Index Terms*—Long Term Evolution (LTE), Radio-over-Fibre (RoF), Fast Fourier Transform (FFT) Optimization**

I. INTRODUCTION

The 4th Generation LTE and LTE-A developed by the 3GPP group is specifically to meet the throughput requirement of the exponentially increased end-user. LTE and LTE-A are going live in 2013 [1], therefore it is important to solve the existing problem while the technologies remains in the development phase. The major problem of LTE and LTE-A technologies are the operating characteristics of eNB in a non line-of-sight (LOS) scenario such as dense urban area where real time data from [2] shows that the user equipment only receives data rate of <20 Mbps with 1 km cell size. Furthermore in [2] a cell extension of only 3.2 km is achieved with the decode and forward RN at the fixed condition of LOS connectivity between eNB and RN. It is essential to extend the cell coverage of a single eNB to the entire urban area which was shown in our earlier work; where a ~31 dB improvement of signal-to-noise ratio (SNR) was observed by adopting an amplifying and forwarding RN with RoF as the interface compared to wireless radio-frequency interface [3].

The LTE and LTE-A is configured with single carrier modulations (SCMs) of QPSK, 16, 64 and 256-QAM. These SCMs are then modulated onto OFDM with scaled FFT sizes of 128, 256, 512 and 1024 [4]. Therefore, it is important to optimize the FFT size because the increment in the FFT size is inversely proportional to the subcarrier frequency which makes the subcarrier more vulnerable to inter-carrier interference (ICI) induced by the DFB based PFC, CD and nonlinear SPM phase distortion. The optical receiver within the RoF system is based on a single photodetector with direct detection (DD) scheme and therefore the LTE signal over RoF will be termed as DD-optical OFDM (DD-OOFDM).

Jansen *et al* [5] and Adhikari *et al* [6] optimized the FFT size in coherent optical-OFDM (CO-OFDM) while taking the linear and nonlinear optical fibre propagation into consideration. These findings showed that the signals are facing higher distortion for FFT size of above 256 and further explains the importance of FFT size optimization [5, 6]. In Pham *et al* [7] DD-OOFDM systems, the optimization of FFT size was investigated only in the linear propagation region of optical fibre where the system OLP was below -7 dBm. Therefore the analysis was not sufficient enough to address the contribution of nonlinear phase noise (PN) to the varying FFT sizes [7]. In this paper, we are proposing and optimizing the DD-OOFDM signal with FFT sizes of 64, 128, 256, 512 and 1024 over the linear and nonlinear optical fibre propagation and most importantly the linear and nonlinear intermixing region of the OLP. Since the objective of this work is to optimize the FFT sizes for RoF link, we are including FFT size-64, in addition to the predefined FFT sizes, to further investigate the channel characteristic for smaller FFT size which provides larger subcarrier frequency and its impact on ICI.

The paper is organized as follows. Section II introduces the system and the associated theoretical models. Section IV presents and discusses the obtained results. Finally, Section V concludes the findings of the paper.

II. System Model

The DD-OOFDM system shown in Fig. 1 is the overview block diagram of LTE-RoF system. At the transmitter, 39, 76, 151, 301 and 601 parallel data streams are generated and mapped into a parallel complex data using QPSK, 16, 64 and 256-QAM modulation formats within SCM module for all the respective number of data. The QPSK, 16, 64 and 256-QAM systems are designed to operate at 200, 400, 600 and 800 Mb/s, respectively, with a channel bandwidth of 100 MHz.

The OFDM modulator module is important because the FFT size scaling takes place in this module during the operation of OFDM modulation. Within this module, the streams are added with 25, 52, 105, 211, 423 zeros to make it 64, 128, 256, 512, and 1024 parallel subcarriers, respectively, to meet LTE and LTE-A requirements [4]. Then inverse FFT (IFFT) is applied to the parallel complex data in order to generate the OFDM symbols and subsequently added with the respective cyclic prefix (CP) within the OFDM modulator module. The symbols are converted into a continuous signal using two digital-to-analogue converter (DAC) modules for the real and imaginary parts of the signal, respectively. The continuous signal is then up-converted to a carrier frequency of 2.6 GHz by a local oscillator (LO) according to the allocated spectrum for LTE and LTE-A in an urban location [1]. The combined real and imaginary electrical signals are then applied to the DFB laser directly to generate OOFDM signals. The direct modulation of DFB induces the PFC. These signals are then coupled into the single mode fibre (SMF). Erbium doped fibre amplifier (EDFA) is utilized for link span, L above 80 km with 15 dB gain and 5 dB noise figure (NF) [8].

At the receiver side, the optical signals are converted into electrical signals via a single photodetector (PD) adopting DD. Identical LOs are used to ensure perfect synchronization between transmitter and receiver modules. The remaining part of the receiver is the reverse process of the transmitter except for the equalization module. The frequency domain equalizer is used for phase distortion compensation induced by PFC, CD and SPM.

The system evaluation is carried out based on the OLP characteristics and the system bit error rate (BER).

A. OFDM Modulator

The output of the OFDM Modulator module in Fig. 1 prior to adding CP can be described as:

$$S(t) = \frac{1}{\sqrt{NC}} \sum_{i=0}^{NC-1} d_i \exp(j2\pi i \Delta f t); \quad (1)$$

where NC is the total number of subcarriers within the OFDM symbol, d_i is the symbol value, and Δf is the subcarrier frequency spacing. In this paper, NC will be varied between 64, 128, 256, 512 and 1024 as mentioned earlier and the Δf will be varying in the range of 1.56 MHz, 781 kHz, 390 kHz, 195 kHz and 97 kHz with respect to the scaling factor of NC. CP is added to the front end of each OFDM symbol to mitigate the inter-symbol interference in the channel. CP is a copy of the last fraction of each respective OFDM symbol with a rate of ¼ of OFDM symbol. Therefore, the modified OFDM symbol with CP, at the output of OFDM modulator can be expressed as:

$$S(t) = \exp(-j2\pi\Delta f T_p) \sum_{i=0}^{NC-1} d_i \exp(j2\pi i \Delta f t); \quad (2)$$

where T_p is the time duration of the CP. At the receiver, CP is removed from the incoming OFDM symbol streams, and FFT is performed on the OFDM symbols within the OFDM demodulator module followed by the frequency domain equalization with the "EQ" module in order to recover the symbols.

B. DFB Model

We have modeled the characteristics of the DFB in the system shown in Fig. 2 for an IM scheme by utilizing the rate of change of carrier density, dN/dt from (3) and photon density, dS/dt from (4) within a DFB laser with respect to the total current injected, I_d. On the other hand, (5) describes the DFB laser output power, P at the DFB facet [9]:

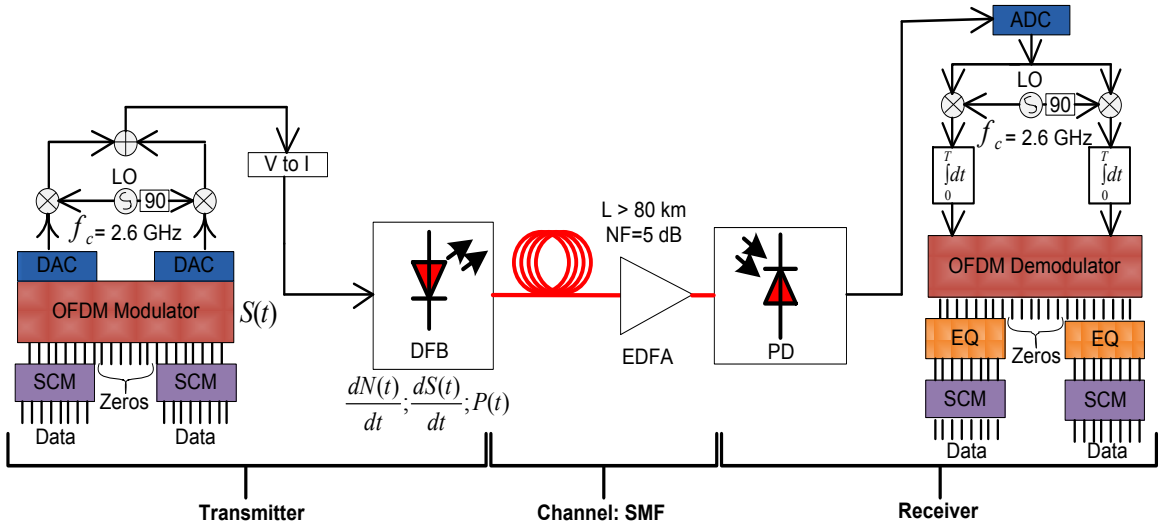

Fig. 1: Overall block diagram of DD-OOFDM. Abbreviations: SCM- Single Carrier Modulation, OFDM- Orthogonal Frequency Division Multiplexing, DAC- Digital-to-Analogue Converter, LO- Local Oscillator, DFB- Distributed Feedback Laser, SMF- Single Mode Fibre, EDFA- Erbium Doped Fibre Amplifier, PD- Photodetector, ADC- Analogue-to-Digital Converter and EQ- Equalizer

$$\frac{dN}{dt} = \frac{I_d}{edwl} - \frac{N}{\tau_c} - G\frac{(N-N_t)}{1+\varepsilon S}S; \quad (3)$$

$$\frac{dS}{dt} = \frac{\Gamma G(N-N_t)}{1+\varepsilon S}S + \frac{\Gamma\zeta N}{\tau_c} - \frac{S}{\tau_p}; \quad (4)$$

$$P = xw_v w_h h\nu \frac{Sc}{2n_g}; \quad (5)$$

where e is the electronic charge, thickness d, width w, and length l. N is the carrier density, τ_c is the linear carrier recombination lifetime. G represents the linear optical gain coefficient, N_t is the transparency carrier density, ε is the nonlinear gain coefficient and S is the photon density. Γ is the mode confinement factor. ζ represents the fraction of spontaneous emission. τ_p is the photon lifetime. χ is the coupling efficiency from the laser chip to the SMF, w_v and w_h are the vertical and horizontal widths of the guided mode power distributions, respectively. $h\nu$ is the photon energy and c presents the speed of light in vacuum. All DFB simulation parameters are adopted from [9]. The continuous 2.6 GHz OFDM signal is used to directly drive the DFB model by coupling it with a bias current of 40 mA because bias current > 37 mA induces smaller PFC [9].

C. SMF

In this work, the FFT size scaling analysis takes place at the linear and nonlinear propagation intermixing region to achieve the optimum power launch condition. The interaction between direct modulated DFB induced PFC and CD that jointly distorts the signal phase can be controlled with proper optimization of the optical launching power which is a switch-like mechanism that controls the SPM. It is known that light propagation through a dispersive and nonlinear fiber channel is governed by the generalized nonlinear Schrödinger equation (NLSE) [10]. The nonlinear phase distortion induced by SPM alone can be expressed as [10]:

$$\phi_{NL}(l, T_N) = -\frac{1-\exp(-\alpha l)}{\alpha}\frac{2\pi}{\lambda}n_2|A(0,T)|^2 \quad (6)$$

where l is the propagation distance, T_N is the normalized time, α is the fibre attenuation, λ is the optical wavelength, n_2 is the nonlinear index and A is the slowly varying optical signal envelope. From (6), we can observe that SPM induced phase distortion is dependent on l and the optical signal peak power (i.e. optical signal envelope).

At 1550 nm transmission window with SMF as the transmission channel, the distortion term of SPM has an opposite phase to the PFC and the CD induced phase distortion. Therefore, the nonlinear induced phase distortion can be taken as an advantage to mitigate the PFC and CD induced power penalty by proper control of the OLP applied to the SMF. However, beyond certain limit which will be shown in the next section, the SPM induced chirp will become the dominant effect.

III. Results and Discussion

The conventional wireless communication aims to achieve a BER of 10^{-5} with coded modulation [11]. Within this work, we aim to achieve the aforementioned BER without coding to enhance the spectral efficiency.

A. Optical power launch analysis

Figs. 2(a), (b), (c) and (d) depict the OLP against the power

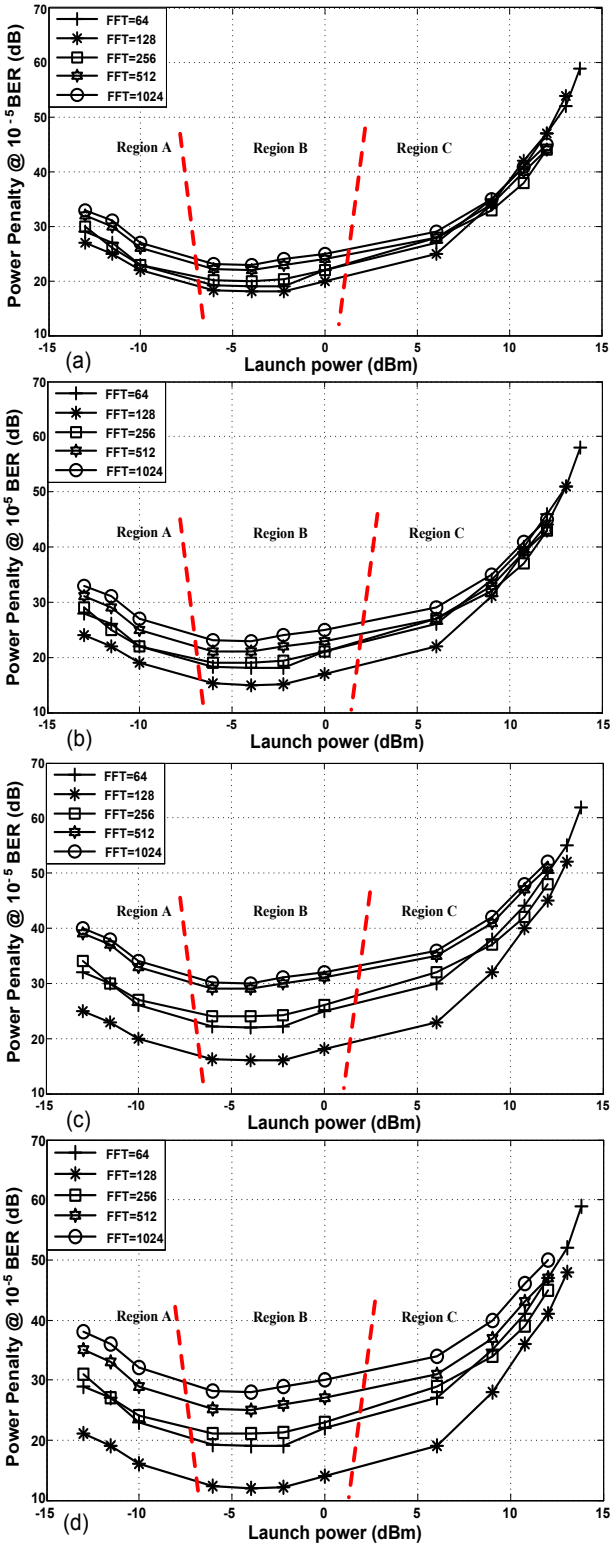

Fig. 2: OLP against power penalty analysis of DD-OOFDM, with (a) QPSK-119 km, (b) 16-QAM-69 km, (c) 64-QAM-57 km and (d) 256-QAM-29 km.

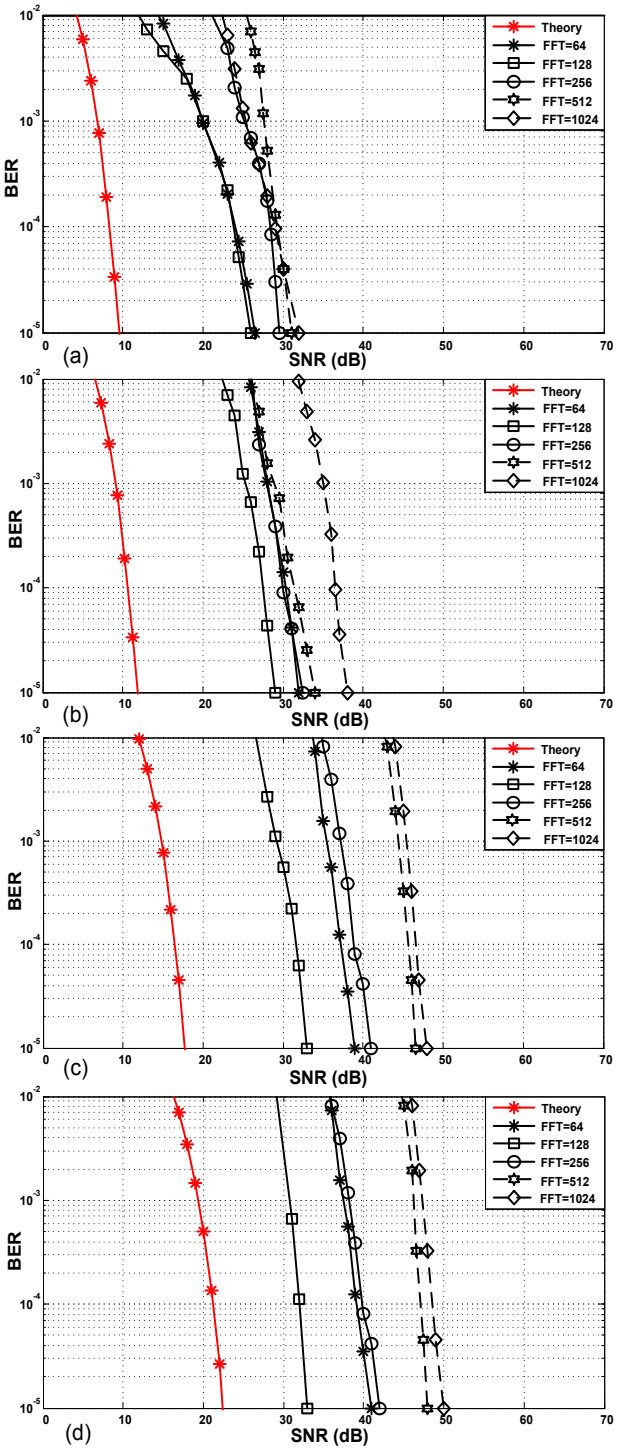

Fig. 3: BER analysis of DD-OOFDM, with (a) QPSK-119 km, (b) 16-QAM-69 km, (c) 64-QAM-57 km and (d) 256-QAM-29 km.

penalty with respect to DD-OOFDM with QPSK, 16-QAM, 64-QAM and 256-QAM, respectively at the facet of the DFB measured with the BER of 10^{-5}. The maximum link spans achieved are ~119 km, ~69 km, ~57 km and ~29 km for QPSK, 16-QAM, 64-QAM and 256-QAM, respectively. In Fig. 2(a), (b), (c) and (d), there are three distinctive regions: **A**) PFC and CD induced power penalty, **B**) optimized OLP from the intermixing effect of SPM with PFC and CD, and **C**) SPM induced power penalty [12]. Region C and more importantly B are not identified in literature [7]. In region B the optimum launch point ranges from ~-6 dBm to ~0 dBm which results in the lowest average power penalty across all the FFT sizes of 20.4 dB, 20 dB, 24.2 dB, and 21.8 dB for QPSK, 16-QAM, 64-QAM and 256-QAM respectively. The QPSK achieves almost identical power penalty with respect to 16-QAM due to the additional noise contribution from EDFA that was specifically used for QPSK only because of the link span is greater than 80 km [8]. The 256-QAM system achieved lower penalty compared to 64-QAM due to the short transmission range of only 29 km compared to 57 km of 64-QAM system. All the systems would not be able to achieve BER of 10^{-5} for transmission of above the aforementioned distances. It is clear from Fig. 2 that Region A induces higher power penalty while significant increase in power penalty can be observed from Region C due to higher launching power that induces higher nonlinear phase distortion as explained earlier with (6). The rest of the analysis will be carried out at -2 dBm OLP which falls in the range of ~-6 dBm to ~0 dBm, the intermixing region.

At the BER of 10^{-5} from Fig 3(a), (b), (c) and (d) of QPSK, 16-QAM, 64-QAM and 256-QAM, respectively, the highest achievable transmission distance, between all the RoF configurations, is ~119 km for QPSK (200 Mb/s) at the lowest SNR of ~27 dB (FFT size-64) and ~26 dB (FFT size-128). In the same QPSK system, FFT-size of 256, 512 and 1024 requires higher SNR of ~29 dB, ~32 dB and ~33 dB, respectively to achieve the transmission distance of 119 km. The fundamental behind this occurrence is that the increase in the FFT size decreases the subcarrier frequency which makes it more susceptible to ICI. From Fig. 3 (b), (c) and (d), we can observe that the FFT size-64 requires higher SNR as the bit rate increases. From 16-QAM, 64-QAM and 256-QAM, the FFT size-64 requires SNR of ~32 dB, ~39 dB, and ~41 dB, respectively compared to FFT size-128 which only requires SNR of ~29 dB, ~33 dB and ~32 dB, respectively. This is because FFT size-64 provides a subcarrier frequency of 1.56 MHz. Therefore the effect of walk-off is higher because the PN will be directly affecting a bigger division from the total channel bandwidth of 100 MHz. As the data rate increases, the allocated data within a subcarrier increases which leads to higher BER and subsequently increases the required SNR.

Fig. 4 presents the summarized output of the FFT size

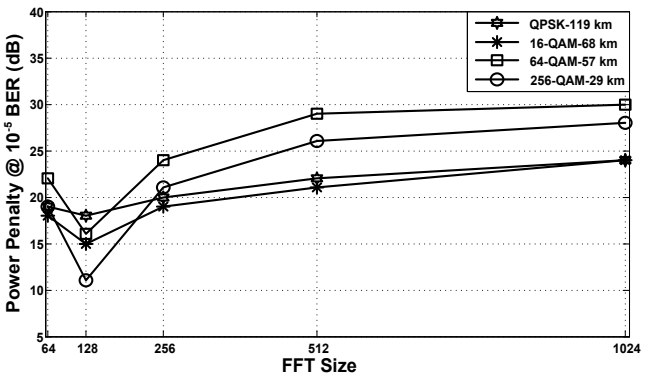

Fig. 4: FFT size against power penalty with optimum FFT size corresponding to lowest power penalty

analysis of DD-OOFDM with QPSK, 16-QAM, 64-QAM and 256-QAM transmitted at the optimized OLP. From Fig. 4, the QPSK DD-OOFDM system achieves almost identical power penalty at FFT size-64 and 128 due to the similar effect of PN at 200 Mb/s with subcarrier frequency spacing of 1.56 MHz and 781 kHz, hence resulting in similar walk off effect. Above this bit rate, FFT size-64 has higher effect due to the higher frequency spacing which is proportional to higher walk off and fundamentally related to the increase in the bit rate within a subcarrier.

The FFT size-128 achieves the lowest power penalty across all modulation schemes shown within Fig. 4. For FFT size>128, the subcarrier spacing is narrower with respect to the increment in subcarrier numbers which will be easily affected by phase distortion that leads to ICI. Finally transmission at the optimum FFT size-128 could provide overall average system efficiency across four modulation schemes with respect to FFT size-64 is 54% and FFT size-256 is 65%.

IV. Conclusion

In this paper, we have optimized the OLP condition with respect to the varying FFT-sizes and the optimum launch region/intermixing region which mostly falls in the range of ~-6 dBm to ~0 dBm for QPSK, 16-QAM, 64-QAM and 256-QAM, respectively. By considering that particular region, further analysis was carried out at -2 dBm OLP. We identified that for FFT size-64, the walk off tolerance gradually decreases with the increase of bit rate for 16-QAM, 64-QAM and 256-QAM. For FFT size≥ 256, the power penalty increases significantly for QPSK, 16-QAM, 64-QAM and 256-QAM due to the vulnerability towards ICI. The finding within this paper is that FFT size-128 provides the minimum power penalty across all aforementioned modulation schemes which means it could provide enough tolerance to walk off from PN and at the same time the subcarrier spacing induces lower probability of ICI.

References

[1] J. Gozalvez, "Long-Term Evolution advanced Demonstrations [Mobile Radio]," *Vehicular Technology Magazine, IEEE,* vol. 6, pp. 4-9, 2011.

[2] T. Wirth, V. Venkatkumar, T. Haustein, E. Schulz, and R. Halfmann, "LTE-Advanced Relaying for Outdoor Range Extension," in *Vehicular Technology Conference Fall (VTC 2009-Fall), 2009 IEEE 70th*, 2009, pp. 1-4.

[3] T. Kanesan, W. P. Ng, Z. Ghassemlooy, and J. Perez, "Radio relaying for long term evolution employing radio-over-fibre," in *Networks and Optical Communications (NOC), IEEE 16th European Conference on*, 2011, pp. 212-215.

[4] U. Barth, "3GPP Long-Term Evolution/ System Architecture Evolution Overview," *Alcatel,* 2006.

[5] S. L. Jansen, A. Al Amin, H. Takahashi, I. Morita, and H. Tanaka, "132.2-Gb/s PDM-8QAM-OFDM Transmission at 4-b/s/Hz Spectral Efficiency," *Photonics Technology Letters, IEEE,* vol. 21, pp. 802-804, 2009.

[6] S. Adhikari, B. Inan, O. Karakaya, W. Rosenkranz, and S. L. Jansen, "FFT optimization for practical OFDM implementations," in *Optical Communication (ECOC), 2011 37th European Conference and Exhibition on*, 2011, pp. 1-3.

[7] D. T. Pham, M.-K. Hong, J.-M. Joo, E.-S. Nam, and S.-K. Han, "Laser phase noise and OFDM symbol duration effects on the performance of direct-detection based optical OFDM access network," *Optical Fiber Technology,* vol. 17, pp. 252-257, 2011.

[8] H. Bao and W. Shieh, "Transmission simulation of coherent optical OFDM signals in WDM systems," *Opt. Express,* vol. 15, pp. 4410-4418, 2007.

[9] X. Zheng, X. Q. Jin, R. P. Giddings, J. L. Wei, E. Hugues-Salas, Y. H. Hong, and J. M. Tang, "Negative Power Penalties of Optical OFDM Signal Transmissions in Directly Modulated DFB Laser-Based IMDD Systems Incorporating Negative Dispersion Fibers," *Photonics Journal, IEEE,* vol. 2, pp. 532-542, 2010.

[10] F. Ramos, J. Marti, V. Polo, and J. M. Fuster, "On the use of fiber-induced self-phase modulation to reduce chromatic dispersion effects in microwave/millimeter-wave optical systems," *Photonics Technology Letters, IEEE,* vol. 10, pp. 1473-1475, 1998.

[11] E. Zehavi, "8-PSK trellis codes for a Rayleigh channel," *Communications, IEEE Transactions on,* vol. 40, pp. 873-884, 1992.

[12] T. Kanesan, W. P. Ng, Z. Ghassemlooy, and J. Perez, "Optimization of Optical Modulator for LTE RoF in Nonlinear Fiber Propagation," *Photonics Technology Letters, IEEE,* vol. 24, pp. 617-619, 2012.